Int. J. Mach. Tools Manufact. Vol. 33, No. 1, pp.89–102, 1993.
Printed in Great Britain

0890–6955/93$6.00 + .00

ASSESSMENT OF CHIP FORMING PATTERNS WITH TOOL WEAR PROGRESSION IN MACHINING VIA NEURAL NETWORKS

Y. L. YAO† and X. D. FANG‡

(*Received* 8 *July* 1991)

Abstract—This paper presents a new method of employing techniques of neural networks to quantify the complicated interrelationship between the change of chip breakability and that of comprehensive wear states, including major flank, crater and minor flank wear. Chip breakability under unworn cutting tools is first predicted through a fuzzy rating system, then updated dynamically as tool wear develops. Change in surface finish with tool wear progression is assessed via the neural networks and finish conditions were used where both chip breakability and surface finish are primary concerns. Both training and testing results show that the method is not only valid and effective, but also provides a feasible means for in-process prediction of chip breakability and surface finish in automated finish-machining systems.

1. INTRODUCTION

EFFECTIVE chip control has been recognized as an important aspect in automated machining systems. Although much work has been done on analysis and prediction of chip forming patterns including chip shapes and chip breaking in machining [1–4], all assume ideal machining conditions, i.e. machining with an *unworn* cutting tool. It is also known that present theories concerning chip formation in machining and available machinability databases are all established based on unworn tools. In actual machining processes, however, the chip forming patterns vary significantly with tool wear progression, thus resulting in unpredictable performance of the machining operation. In this sense, a truly effective chip control system should not only be capable of predicting chip forming patterns off-line but also updating them on-line as tool wear develops in the machining process.

During the machining process, tool wear formed at different tool faces alters the original tool configuration/geometry, which, in turn, greatly influences chip forming patterns. In order to assess chip forming patterns with wear progression, an effective estimation strategy for tool wear at different tool faces is a prerequisite. Many methods have been developed [5–10], among which, dispersion analysis of 3-D dynamic cutting force derived from multivariate time series models has proven particularly effective for comprehensive tool wear estimation, i.e. more than one type of wear can be estimated simultaneously [9], thus providing a possible basis for predicting chip forming patterns during tool wear progression.

Since the interrelationship between chip forming patterns and tool wear progression is extremely complex and the present machining theories are inadequate to describe it analytically, a certain form of "black-box" approach becomes appealing even inevitable for tackling the problem. One such approach, neural networks, has been applied recently in machining process monitoring and control, such as tool wear monitoring [11–13] and optimization of machining process [14]. Neural networks provide a new approach to resolve a complicated problem through the way of learning by

† School of Mechanical and Manufacturing Engineering, University of New South Wales, P.O. Box 1, Kensington, NSW 2033, Australia. Author to whom correspondence should be addressed.
‡ Department of Mechanical Engineering, University of Wollongong, P.O. Box 1144, Wollongong, NSW 2500, Australia.

being shown and synthesizing knowledge from the observed input and output variables of the process under investigation.

For the chip forming pattern problem, chip shapes produced are observable and readily collectable, while tool wear can be estimated with higher certainties by the monitoring strategy developed [9]. Therefore, employing neural network techniques, which model a complicated process by extracting knowledge largely based on experimental input–output data, would be feasible to correlate dynamic chip forming patterns with tool wear progression. In addition, a network algorithm can be implemented on-line, once it is trained off-line.

In this paper, assessing chip breaking/shapes under the condition of an unworn tool is first summarized, which provides the initial estimation of chip forming patterns. Neural networks are then trained based on the recorded data of chip breakability/surface roughness in finish-machining with tool wear progression. The latter is characterized by four features extracted from multivariate time series models of 3-D dynamic cutting force signals. Using the results derived from neural network modelling, together with the comprehensive tool wear estimation reported in Ref. [9], on-line assessment of machining performance is achieved, which includes chip breaking/chip shapes, surface finish and tool wear states.

2. ASSESSMENT OF CHIP CONTROL FOR UNWORN TOOLS†

A series of machining experiments was conducted to set up a basic chip database for assessment of chip breaking/shapes for fresh or unworn tools. This effectively provides initial conditions for in-process assessment when tool wear is taking place.

It has been shown that the quantitative description of chip forming patterns can be achieved through a fuzzy membership function, ranging from 0 to 1 [4], where fuzzy membership values, μ (representing chip breakability ratings), are assigned to the chip shapes/sizes obtainable, based on the relative ease/difficulty of producing them. Table 1 shows some representative chips obtained from machining, with larger membership values representing better chip breakability.

TABLE 1. MEMBERSHIP VALUES FOR MOST COMMON CHIP SHAPES/SIZES

Tubular Chips	Large Diameter 0.10	Snarled 0.28	Continuous Long 0.35	Broken Long 0.43	Medium 0.46–0.48	Short 0.64
Ribbon Chips	Snarled 0.20	Long 0.30	Small Snarled 0.3–0.45			
Helical Chips	Large Diameter 0.08	Snarled 0.20	Continuous Long 0.30	Broken Long 0.38	Medium 0.44–0.46	Short 0.60
Cork Screw Chips	Snarled 0.25	Continuous Long 0.32	Broken Long 0.41	Medium 0.45–0.47	Short 0.62	
Spiral Chips	Wavy 0.44–0.48	Few Turns 0.42–0.48	Full Turn 0.65–0.67	Flat 0.57–0.60	Conical 0.67–0.70	
Arc Chips	Up-curl 0.88–0.92	Side-curl 0.85–0.90	Connected 0.92–0.95			
String Chips	Continuous Long 0.35	Broken Long 0.42	Medium 0.49	Short 0.64		
Tooth-Edged Chips	Long 0.28	Short 0.60	Side-curl Arc 0.86	Connected Arc 0.92		

†This part is largely based on Ref. [4] and is included for completeness.

3. DESCRIPTIONS OF MACHINING EXPERIMENTS

3.1. *Machining conditions*

A series of machining experiments concerning chip breaking/chip shapes, surface finish and tool wear was carried out under the finish-machining conditions to obtain the data needed for training and testing the neural networks to be established. Shown in Table 2 are the machining conditions used in the experiments. The cutting conditions are organized into two groups, i.e. training and testing. The degraded tool tests, namely using a relatively softer tool as recommended in Ref. [15], are adopted to shorten the time-consuming and costly tool wear experiments.

3.2. *Investigation of comprehensive tool wear patterns*

Patterns of major flank, crater and minor flank wear were investigated as they reflect the comprehensive wear situation and significantly influence tool configuration/geometry and the surface quality of a finished product. The wear was quantitatively determined by joint use of scanning electron microscopy (SEM), a surface measurement instrument and a coordinate measuring machine (CMM). Figure 1 plots typical measurement results of major flank wear VB, crater wear (depth) KT and minor flank wear VB' for training cutting condition 1, to show the development patterns of these three types of tool wear.

3.3. *Chip breakability assessment*

Chip breakability was described by using the fuzzy membership function according to the chip shapes/sizes produced in the machining process. Figure 2 illustrates the change of chip shapes/sizes with cutting time under training cutting condition 1 and Table 3 gives the description of these chips and the corresponding fuzzy membership values assigned.

As seen from Fig. 2 and Table 3, it is clear that tool wear has a significant effect on chip forming behaviour. This is largely due to the fact that when tool wear develops, the tool geometry changes accordingly. In the initial stage of machining, long and continuous chips form because the tool insert used has no chip breaker. With the increase of machining time, tool wear causes the change of tool configuration/geometry. In particular, the formation of crater wear on the tool rake face acts as a groove-type chip breaker and thus increases chip breakability. As crater wear grows further its effect as the chip breaker becomes more significant until a fully-utilized chip breaker

TABLE 2. MACHINING CONDITIONS USED IN THE EXPERIMENTS

Machine tool	Colchester Mascot 1600 (9.3 kW)
Tool insert type	TNMA 160408F (no chip breaker)
Tool material	Carbide : Grade 883, SECO
Tool geometry	0°, 5°, −6°, 90°, 60°, 0.8°
Work material	AISI4140 (BHN=275–320)
Depth of cut	d=0.5 mm

Cutting Speed and Feed

Training group	Testing group
1. V = 115 m/min f = 0.10 mm/rev	1. V = 140 m/min f = 0.12 mm/rev
2. V = 145 m/min f = 0.10 mm/rev	2. V = 165 m/min f = 0.06 mm/rev
3. V = 145 m/min f = 0.06 mm/rev	3. V = 190 m/min f = 0.06 mm/rev
4. V = 205 m/min f = 0.06 mm/rev	4. V = 130 m/min f = 0.15 mm/rev
5. V = 170 m/min f = 0.10 mm/rev	
6. V = 160 m/min f = 0.15 mm/rev	

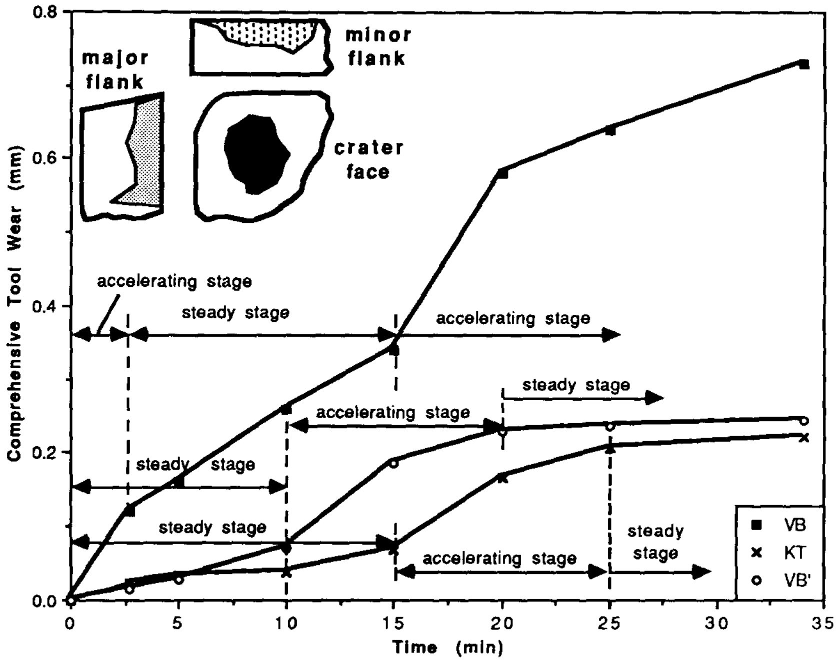

FIG. 1. Development patterns of comprehensive tool wear.

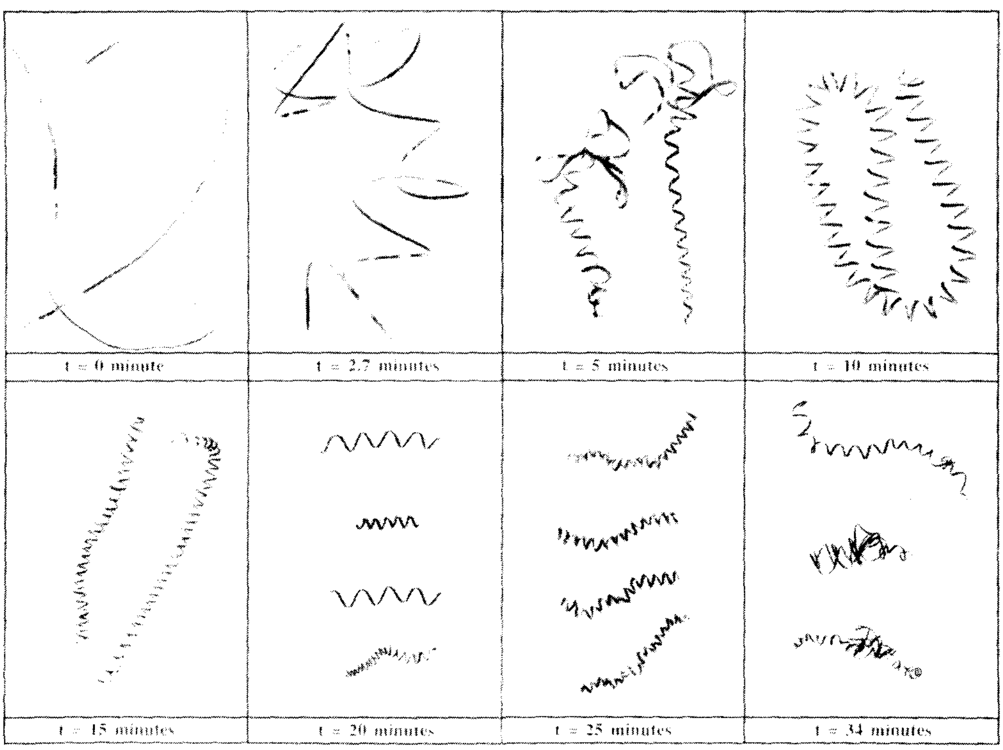

FIG. 2. Change of chip shapes/sizes with tool wear progression.

is realized which breaks chips in the most effective way as seen at t = 20 min. Further growth of crater wear oversizes the chip breaker, resulting in the increase of chip curling curvature which lowers chip breakability. The change of chip breakability as tool wear develops has been observed consistently under all cutting conditions used, as

TABLE 3. CHIP FORMING BEHAVIOUR IN MACHINING PROCESS DURING TOOL WEAR

Time (min)	Chip shapes/sizes	Chip breakability (membership value)
0	long and continuous ribbon chips	0.25
2.7	curved ribbon chips	0.30
5	combination of ribbon and continuous cork-screw chips	0.32
10	long and continuous cork-screw chips	0.35
15	long but broken cork-screw chips	0.41
20	short to medium size chips	0.58
25	distorted medium size chips	0.46
46	heavily distorted long but broken chips	0.42

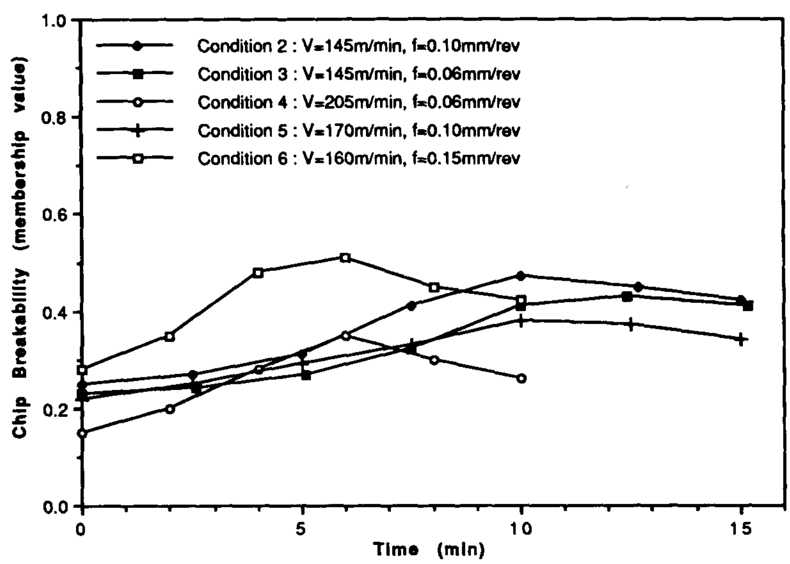

FIG. 3. Change of chip breakability under training cutting conditions 2–6.

shown in terms of fuzzy membership values in Fig. 3 for training cutting conditions 2–6.

Although the above analysis clearly confirms the interrelationship between chip forming patterns and tool wear progression, its analytical modelling proves prohibitively difficult, even impossible. In order to predict the chip forming patterns, a quantitative description of the relation is required. This motivated the introduction of neural networks to model the relationship.

3.4. *Surface finish assessment*

Surface finish was assessed in terms of the arithmetic mean deviation, R_a, with the use of a portable surface measurement instrument. Although surface finish can be predicted theoretically with some accuracy, its development heavily depends on the severity of tool wear during the machining process, as shown in Fig. 4 for training cutting condition 1. Compared with the tool wear development shown in Fig. 1, it is noticeable that the significant increase of surface roughness corresponds to the acceleration stage of minor flank wear. Similar results were obtained under training cutting conditions 2–6.

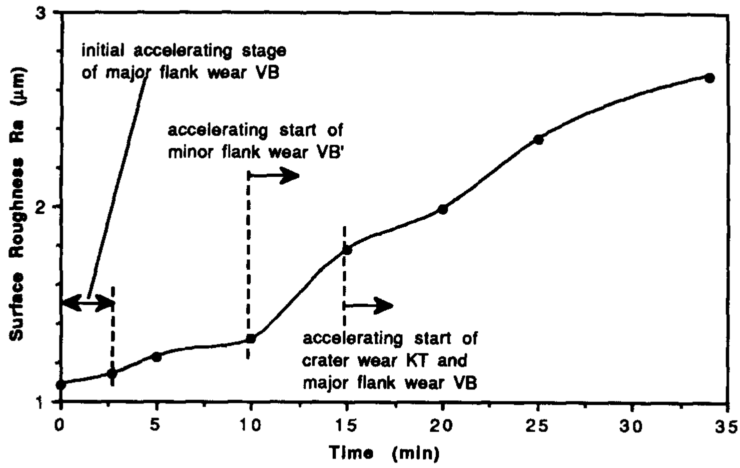

FIG. 4. Change of surface finish with tool wear rates for training cutting condition 1.

4. FEATURE EXTRACTION FROM 3-D DYNAMIC CUTTING FORCES

Various types of tool wear development have been reliably correlated with four features extracted from dynamic components of 3-D cutting forces [9]. The results are summarized below.

A trivariate autoregressive time series vector (ARV) model [16] was developed to analyse the dynamic relationships among the 3-D cutting force data sampled from the machining process. An ARV model with nth order can be expressed as:

$$\mathbf{X}_t = \sum_{k=1}^{n} \Phi_k \mathbf{X}_{t-k} + \mathbf{a}_t \tag{1}$$

where $\mathbf{X}_t = (X_{1t}, X_{2t}, X_{3t})^T$, $X_{1t} = F_{xt}$ = feed force, $X_{2t} = F_{yt}$ = thrust force and $X_{3t} = F_{zt}$ = main cutting force. The values of Φ_k are autoregressive coefficients describing the instantaneous dynamics of the machining process; $\mathbf{a}_t$ is the independent random vector. The model order n may be determined by the F-test [16] or Akaike's Information Criterion (AIC) [17].

Since 3-D dynamic cutting force signals are to be analysed to estimate more than one type of tool wear, a method, which is capable of singling out particular features in the signals corresponding to particular types of tool wear, must be used. Dispersion analysis has proven to be effective to quantify the relationships [9,18,19]. The calculation of dispersion is associated with the eigenvalues λ_i (i=1, 2, ..., n for each time series) of the established ARV models, as shown below:

$$d_i = g_i \sum_{k=1}^{n} \frac{\sigma_a g_k}{1-\lambda_i\lambda_k} \tag{2}$$

where g_i is determined as follows:

$$g_i = \frac{\lambda_i^{n-1}}{\prod_{k=1,k\neq i}^{n} (\lambda_i-\lambda_k)}. \tag{3}$$

The dispersion percentage, D_i, describes the contribution of the roots or ultimately the frequencies in the series to the series variation γ_0 and is given as:

$$D_i = \frac{d_i}{\gamma_0}. \tag{4}$$

The eigenvalues appearing in complex conjugate pairs are found to be of particular interest because they contribute to the oscillating variation of the process. Two dominant percentage dispersions, D_i, one in low frequency (LF) related to the idle frequencies of machine-tool and the other in high frequency (HF) related to the natural frequencies of the tool-holder/dynamometer system, are found to exhibit patterns in agreement with wear rate patterns including major flank wear VB, crater wear KT and minor flank wear VB' shown in Fig. 1 [9]. In summary, the relationship between wear rate patterns and dispersion development patterns is shown in Fig. 5 based on Ref. [9].

5. ARCHITECTURE OF NEURAL NETWORKS

5.1. *Neural network techniques used*

By imitating the computational architecture of human brains and implementing it into software/hardware, neural networks are capable of learning to recognize non-linear and complicated input–output relationships. Back-propagation (BP) is the most widely used learning algorithm for multilayered feed-forward neural networks [20–22]. BP neural networks can be used to attack any problems that require pattern mapping, i.e. given the input pattern, the network produces the associated output. Once the network has learned the pattern mapping from the input–output training set, for any new or previously unpresented input it will be capable of producing an output pattern based on the knowledge derived from the recognized input–output relationship.

The typical BP neural network employs one hidden layer of perceptron neurons fully connected through weights to the input and output layers. The significance of using a hidden layer is that it allows the non-linear mappings between input and output patterns. Shown in Fig. 6 is a three-layer neural network with N inputs, M hidden neurons and L output neurons.

In Fig. 6, the forward propagation takes place first after an input pattern is presented at the input layer. The errors, i.e. the differences between the output pattern (O_j, j=1, 2, ..., L) and target pattern (T_j, j=1, 2, ..., L) are calculated for all neurons in the output layer and propagated back through the network to update their coming weights. Next, an error value is calculated for all the neurons in the hidden layer and the weights are adjusted for all interconnections coming from the input layer. This process is repeated until the output pattern is close enough to the target pattern or until the error is within the convergence criterion determined in advance. The bias is connected to each neuron in the hidden and output layers and is used to adjust the activation threshold of the perceptron neurons during the training process. The function of a

TOOL WEAR TYPES	TOOL WEAR RATE PATTERNS			DESCRIPTIONS OF DISPERSION DEVELOPMENT PATTERNS
	Stage I	Stage II	Stage III	
major flank wear (VB)	accelerating	steady	accelerating	D_x(LF) of feed force
crater wear (KT)	steady	accelerating	steady	D_y(HF) of thrust force
minor flank wear (VB')	steady	accelerating	steady	D_x(HF) of feed force D_z(HF) of main cut ting force

FIG. 5. A typical relationship between tool wear and dispersion patterns.

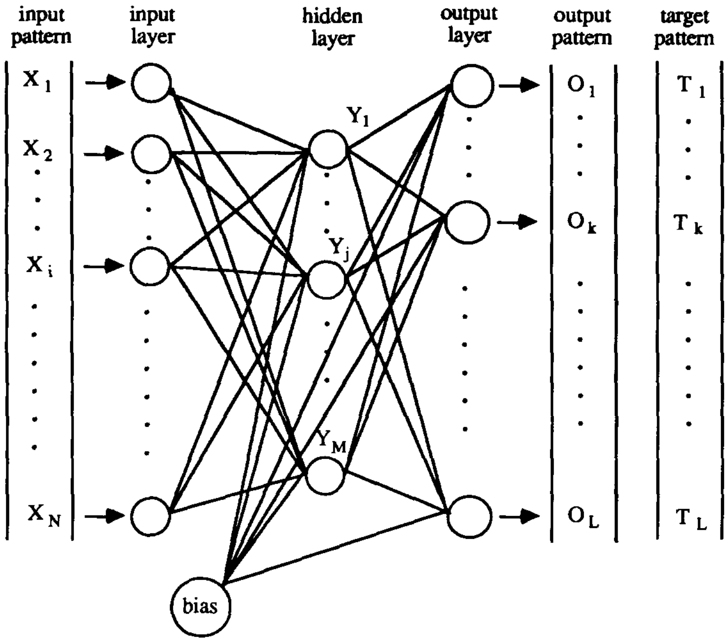

FIG. 6. Back-propagation neural network with one hidden layer.

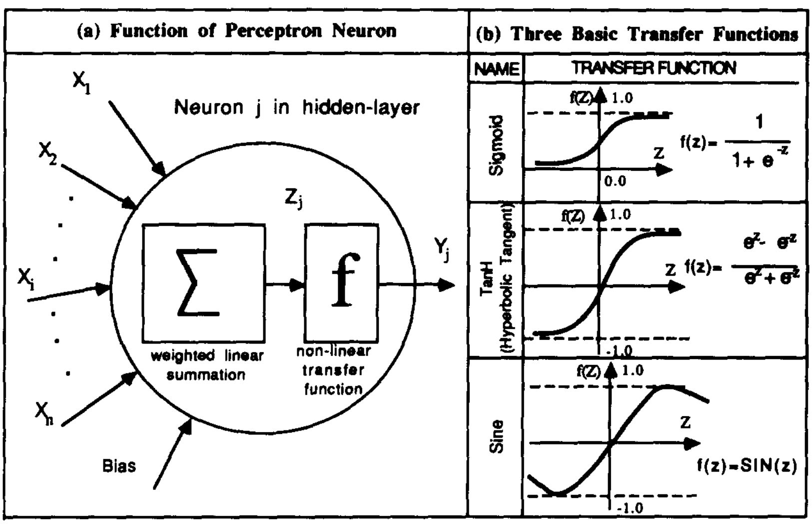

FIG. 7. Algorithm of neural networks.

neuron in the hidden and output layers can be shown in Fig. 7(a) where the total input X_1, ..., X_n to neuron j is a weighted linear summation, i.e.

$$Z_j = \sum_{i=1}^{n} W_{ji} \cdot X_i + B_j \tag{5}$$

where W_{ji} is the weight from the ith input to neuron j and B_j is the bias of the neuron j. Then, a real output value from neuron j is activated by a non-linear transfer function $f(Z_j)$:

$$Y_j = f(Z_j) = f\left(\sum_{i=1}^{n} W_{ji} \cdot X_i + B_j\right). \tag{6}$$

There are many transfer functions which might be implemented in the BP neural network that only require the functions be differentiable everywhere [21]. Figure 7(b) describes three commonly used non-linear transfer functions.

5.2. *Selection of input features*

The appropriate selection of input features is vital to the success of neural networks and depends on the thorough understanding of the problem in question. As described before, chip breakability and surface finish change with tool wear progression, and therefore the features selected should be sensitive to the specific wear types which influence the chip breakability and surface finish. Major flank wear and crater wear (crater depth) significantly change the tool configuration/geometry thus resulting in the change of chip breakability, while minor flank wear is the dominant factor influencing the surface quality of a finished product [9]. Since the dispersion patterns derived from ARV models are sensitive to the rate of the above-mentioned wear types, four associated dispersion features, i.e. the low frequency (LF) dispersion $D_x'(\mathrm{LF})$ of the feed force and the high frequency (HF) dispersion $D_x'(\mathrm{HF})$ of the feed force, $D_y'(\mathrm{HF})$ of the thrust force and $D_z'(\mathrm{HF})$ of the main cutting force are selected as the input features representing effects of tool wear on chip breakability and surface finish.

In addition, an initial condition for assessing chip forming patterns is required. As summarized in section 2 above, assessment of chip shapes/sizes for unworn tools is achieved based on a basic chip database and in terms of a fuzzy membership value, μ. This value is selected as the fifth feature. Two machining parameters, cutting speed and feed, are also selected as the input features due to their close relationship with chip breakability and surface finish. Figure 8 shows the schematic diagram of feature selection, and Table 4 lists the input–output data under training cutting conditions 1–3 as representatives.

In Table 4, $\mu_i(k)$ and $\mu_o(k)$, $k = 1,2, \ldots$, represent the input and output of chip breakability, respectively, whilst:

$$\mu_i(0) = \text{predicted value from the basic chip database; and} \qquad (7)$$

$$\mu_i(k) = \mu_o(k-1).$$

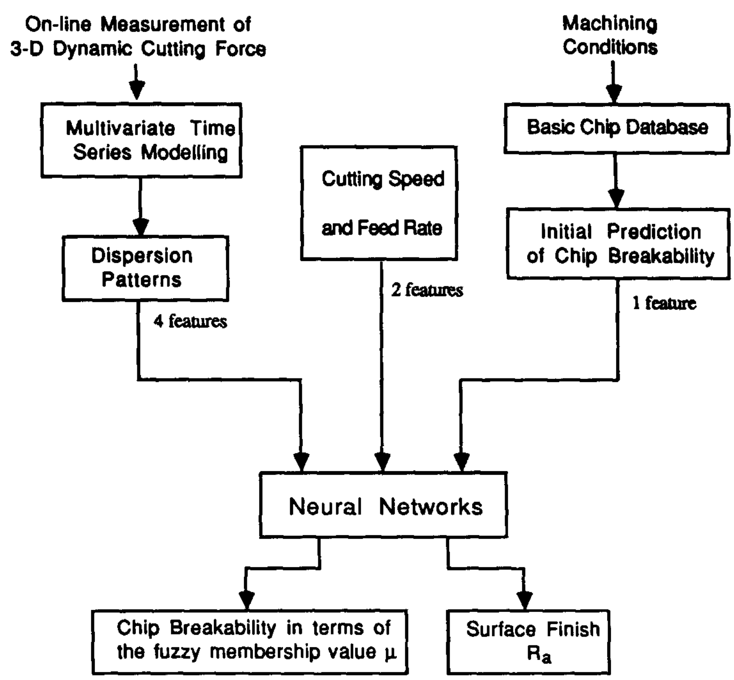

FIG. 8. Feature selection for neural networks.

TABLE 4. THE TRAINING DATA UNDER TRAINING CUTTING CONDITIONS 1–3

	Feed (mm rev^{-1})	Speed (m min^{-1})	Input features: D_x'(LF) (min^{-1})	D_x'(HF) (min^{-1})	D_y'(HF) (min^{-1})	D_z'(HF) (min^{-1})	$\mu_i(k)$	Outputs: $\mu_o(k)$	R_a (μm)
Cutting Condition 1	0.1	115	−4.91	3.22	1.50	1.47	0.25	0.25	1.09
	0.1	115	−3.89	2.52	1.31	1.15	0.25	0.30	1.14
	0.1	115	−3.03	1.92	1.14	0.87	0.30	0.32	1.23
	0.1	115	−1.15	0.62	0.78	0.27	0.32	0.35	1.32
	0.1	115	0.73	−0.68	0.42	−0.33	0.35	0.41	1.78
	0.1	115	2.61	−1.98	0.06	−0.93	0.41	0.58	1.99
	0.1	115	4.49	−3.28	−0.30	−1.53	0.58	0.46	2.35
	0.1	115	7.78	−5.62	−0.95	−2.61	0.46	0.42	2.68
Cutting Condition 2	0.1	145	−5.29	3.83	5.22	4.01	0.25	0.25	1.04
	0.1	145	−3.11	2.31	3.84	2.79	0.25	0.27	1.12
	0.1	145	−1.01	0.78	2.54	1.56	0.27	0.31	1.27
	0.1	145	1.01	−0.75	1.29	0.34	0.31	0.41	1.64
	0.1	145	3.11	−2.27	−0.01	−0.89	0.41	0.47	1.88
	0.1	145	5.13	−3.92	−1.26	−2.21	0.47	0.45	2.08
	0.1	145	7.48	−5.32	−2.71	−3.34	0.45	0.42	2.27
Cutting Condition 3	0.06	145	−8.50	4.06	4.89	2.87	0.23	0.23	1.00
	0.06	145	−5.80	2.71	3.88	2.06	0.23	0.24	1.06
	0.06	145	−3.20	1.41	2.90	1.29	0.24	0.27	1.14
	0.06	145	−0.70	0.16	1.97	0.55	0.27	0.32	1.35
	0.06	145	1.90	−1.14	0.99	−0.23	0.32	0.41	1.73
	0.06	145	4.40	−2.39	0.05	−0.97	0.41	0.43	1.92
	0.06	145	7.30	−3.84	−1.04	−1.84	0.43	0.41	2.13

Equation (7) assumes the fact that no sudden change in chip breakability will occur as tool wear is normally a process of gradual progression. It is therefore reasonable to use the output of chip breakability from the neural network at previous time interval $\mu_o(k-1)$ as the value of current input $\mu_i(k)$, with the initial chip breakability $\mu_i(0)$ from the established basic chip database for unworn tools.

6. ANALYSIS OF RESULTS FROM NEURAL NETWORKS

6.1. *Training strategy with neural networks*

The objective of using neural networks is to predict the development patterns of chip breakability and surface finish at different wear states. Therefore, the input data should be presented to the neural network by group in order to learn the development trend of chip breakability and surface finish during the process of tool wear. The training task in this work is to have the neural network learn the mappings from the given input patterns to the desired output patterns under the training cutting conditions 1–6 (Table 2) that contain 41 samples in total. As the system under investigation contains only seven inputs and two outputs, one hidden layer is sufficient to establish an effective neural network [22].

How to select the optimum number of hidden neurons is a critical yet complicated issue in back-propagation networks [23,24]. In this work, an experimental approach was taken to the selection of the number of hidden neurons. The training procedure started with 7 and ended with 14 hidden neurons in line with the number of inputs/outputs. Due to lack of knowledge about which transfer function would give the best performance for the problem in question, three common transfer functions, i.e. sigmoid, hyperbolic tangent (TanH) and sine, are used in each training process. As the training time is not important in the off-line stage for the size of neural networks concerned, the training process did not stop until no further improvement was observed.

6.2. *Analysis of results for training and testing effects*

A Macintosh-based package, NeuralWorks Professional II, was used to establish the neural networks. Figure 9 shows the RMS errors for all the neural networks trained with different numbers of hidden neurons and different transfer functions. It is seen that 12 hidden neurons is the minimum RMS error achieved for all three transfer functions. This is in agreement with Ref. [11] where the experimental results show that up to a certain number, further increase of hidden neurons does not always lead to a better performance of neural networks. From Fig. 9, it can also be concluded that among the three transfer functions, TanH gives the minimum RMS errors, 0.014, which should be considered as sufficiently close to zero [22].

The training effects of the selected 7–12–2 (i.e. 7 inputs, 12 hidden neurons and 2 outputs) neural networks with the TanH transfer function are shown in Fig. 10 with training cutting conditions 1 and 2 as representatives. The results indicate that the selected neural network is capable of learning the mappings between the given input patterns and the desired output patterns with quite acceptable accuracy.

Four groups of testing cutting conditions shown in Table 2, which were not used in training of the neural network, are used to test the performance of this 7–12–2 network. Figures 11(a) and (b) show the comparisons between the actual outputs and the predicted network outputs for chip breakability and surface finish, respectively. Although the results, as expected, are slightly poorer than those during the training shown in Fig. 10, they should be considered close enough to describe the in-process relationship between chip breakability/surface finish and tool wear states under finish-machining conditions.

7. CONCLUSIONS

The integration of chip forming patterns with tool wear progression is extremely complicated. No effective theories at present can describe their interrelationship analytically. Thus neural networks, which largely rely on input–output data have proven effective for the problem under investigation.

With the appropriate selection of a neural network structure and activation transfer function, the mappings between the given input and output patterns can be quite precisely achieved through training. Thus, predictions of chip breakability and surface

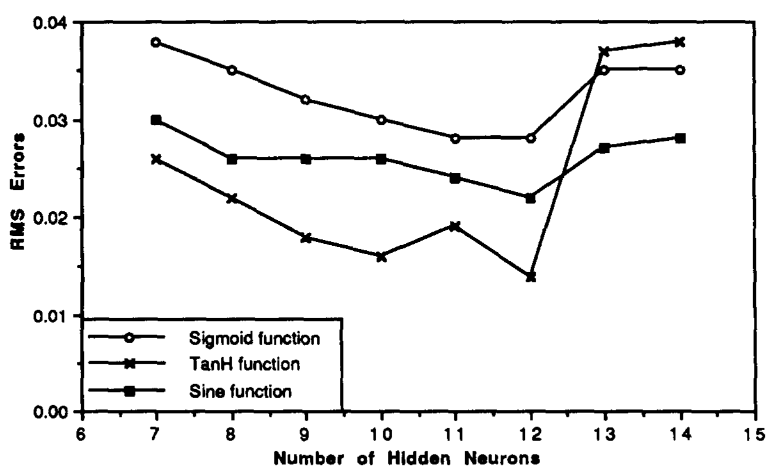

FIG. 9. Effect of the number of hidden neurons for three transfer functions.

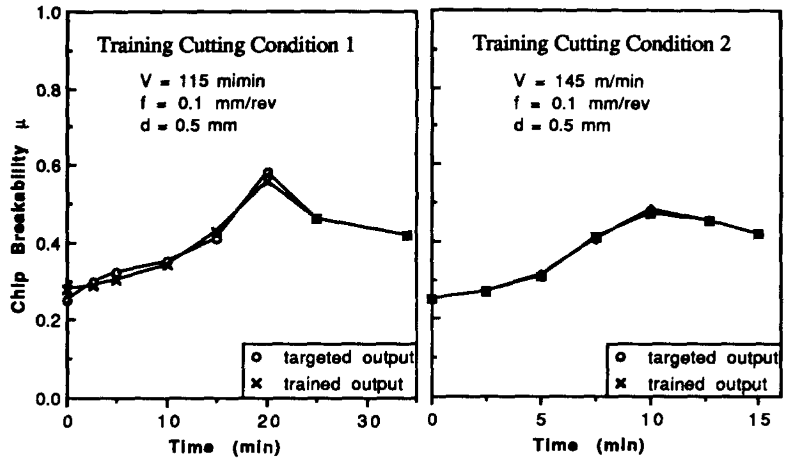

(a) Effect of Chip Breakability

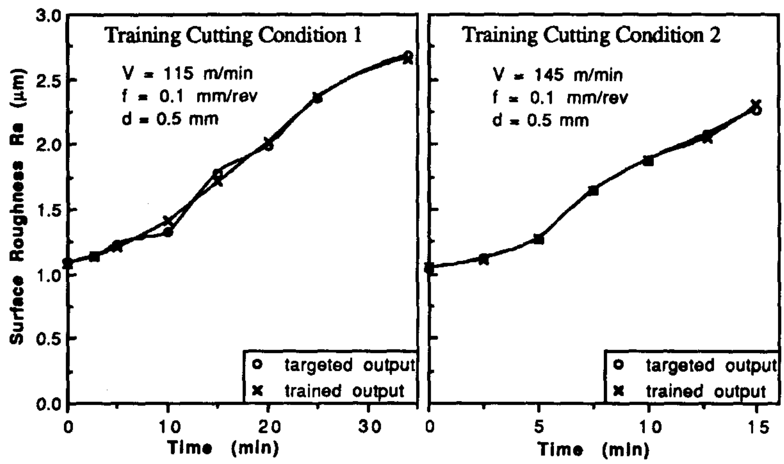

(b) Effect of Surface Finish

FIG. 10. Evaluation of training effects on (a) chip breakability and (b) surface finish.

finish for any new input data, which were not used in training and may come from different cutting conditions, can be achieved with quite acceptable accuracy.

Although the results of this work are only for a flat-faced tool, they can be extended to complicated tool configurations by using the methodology presented in this paper. The method may be extended to rough-machining conditions as well where power consumption has to be included for its critical effect on change of machining performance with tool wear progression.

Integration of chip forming pattern prediction, comprehensive tool wear estimation as well as surface finish, through neural networks provides an effective means for online assessment of machining performance in automated machining systems.

Acknowledgements—The authors gratefully acknowledge support from the Australian Research Council.

REFERENCES

[1] I. S. JAWAHIR, A survey and future predictions for the use of chip breaking in unmanned systems, *Int. J. Adv. Mfg Technol.* **3**, 87–104 (1988).
[2] K. NAKAYAMA and M. OGAWA, Basic rules on the form of chip in metal cutting, *Ann. CIRP* **27**, 17–21 (1978).
[3] K. NAKAYAMA, Chip control in metal cutting, *Bull. Jpn Soc. Prec. Engng* **18**, 97–103 (1984).

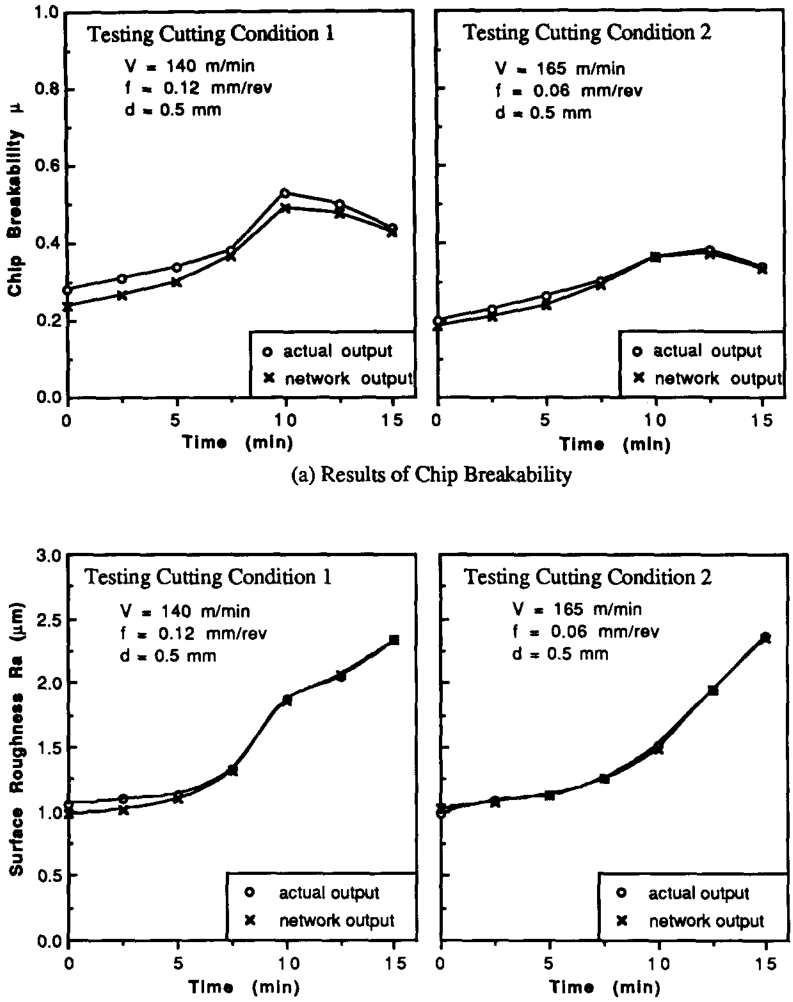

(a) Results of Chip Breakability

(b) Results of Surface Finish

FIG. 11. Neural network performance in predicting (a) chip breakability and (b) surface finish.

[4] X. D. FANG and I. S. JAWAHIR, An expert system based on a fuzzy mathematical model for chip breakability assessments in automated machining, *Proc. Int. Conf., ASME, MI'90*, Atlanta, Georgia, U.S.A., Vol. IV, pp. 31–37 (1990).

[5] D. LI and J. MATHEW, Tool wear and failure monitoring techniques for turning—a review, *Int. J. Mach. Tools Manufact.* **30**, 579–598 (1990).

[6] J. TLUSTY, A critical review of sensors for unmanned machining, *Ann. CIRP* **32**, 563–572 (1983).

[7] H. K. TOENSHOFF, Developments and trends in monitoring and control of machining processes, *Ann. CIRP* **37**, 611–622 (1988).

[8] X. D. FANG and Y. YAO, Expert system-supported on-line tool wear monitoring, *Proc. Int. Conf. Artificial Intelligence in Engng—AIE'90*, Sponsored by I.E.E. (UK)., Kuala Lumpur, Malaysia, pp.77–84 (1990).

[9] Y. YAO, X. D. FANG and G. ARNDT, Comprehensive tool wear estimation in finish-machining via multivariate time-series analysis of 3-D cutting forces, *Ann. CIRP* **39**, 57–60 (1990).

[10] X. D. FANG, Y. YAO and G. ARNDT, Tool wear estimation by multidimensional autoregressive spectral analysis, *Proc.* 1990 *Pacific Conf. on Mfg*, Sydney and Melbourne, Australia, Vol. 2, pp. 834–841 (1990).

[11] D. A. DORNFELD, Neural network sensor fusion for tool condition monitoring, *Ann. CIRP* **39**, 101–105 (1990).

[12] S. RANGWALA and D. DORNFELD, Sensor integration using neural networks for intelligent tool condition monitoring, *Trans. ASME J. Engng Ind.* **112**, 219–228 (1990).

[13] G. CHRYSSOLOURIS and M. DOMROESE, Sensor integration for tool wear estimation in machining, *Proc. WAM/ASME, Symp. Sensors Controls Mfg*, pp. 115–123 (1988).

[14] S. RANGWALA and D. DORNFELD, Learning and optimization of machining operations using computing abilities of neural networks, *IEEE Trans. Systems, Man and Cybernetics* **19**, 299–314 (1989).

[15] B. MILLS and A. H. REDFORD, *Machinability of Engineering Materials*. Elsevier Applied Science, Barking, U.K. (1983).
[16] S. M. PANDIT and S. M. WU, *Time Series and System Analysis with Applications*. Wiley, New York (1983).
[17] R. H. JONES, Multivariate autoregression estimation using residuals, in *Applied Time Series Analysis*, pp. 139–162. Academic Press Inc., New York (1978).
[18] Y. YAO, X. D. FANG and G. ARNDT, On-line estimation of groove wear in the minor cutting edge for finish-machining, *Ann. CIRP* **40** (1991).
[19] Y. YAO, X. D. FANG and R. RUDZIEJEWSKI, Analysis of dynamic components of 3-D cutting forces in oblique machining, *Proc. 5th Int. Conf. Mfg Engng*, Wollongong, Australia, Vol. 2, pp. 349–353 (1990).
[20] D. RUMELHART and J. MCCLELLAND, *Parallel Distributed Processing*, Vol. 1. MIT Press, Cambridge, MA (1986).
[21] P. D. WASSERMAN, *Neural Computing: Theory and Practice*. Van Nostrand Reinhold, New York (1989).
[22] J. E. DAYHOFF, *Neural Network Architectures*. Van Nostrand Reinhold, New York (1990).
[23] S. C. HUANG and Y. F. HUANG, Bounds on the number of hidden neurons in multilayer perceptrons, *IEEE Trans. Neural Networks* **2**, 47–55 (1991).
[24] S. Y. KUNG and J. N. HWANG, Bounds on the number of hidden neurons in multilayer perceptrons, *Proc. IEEE Int. Conf. on Neural Networks*, San Diego, California, Vol. I, pp. 363–370 (1988).